J Mol Model (2013) 19:247–253
DOI 10.1007/s00894-012-1538-5

ORIGINAL PAPER

A new interaction mechanism of $LiNH_2$ with MgH_2: magnesium bond

Xin Yang · Qingzhong Li · Jianbo Cheng · Wenzuo Li

Received: 3 June 2012 / Accepted: 16 July 2012 / Published online: 7 August 2012

Abstract Quantum chemical calculations were performed for $LiNH_2$–HMgX (X=H, F, Cl, Br, CH_3, OH, and NH_2) complexes to propose a new interaction mechanism between them. This theoretical survey showed that the complexes are stabilized through the combinative interaction of magnesium and lithium bonds. The binding energies are in the range of 63.2–66.5 kcal mol^{-1}, i.e., much larger than that of the lithium bond. Upon complexation, both Mg–H and Li–N bonds are lengthened. Substituents increase Mg-H bond elongation and at the same time decrease Li-N bond elongation. These cyclic complexes were characterized with the presence of a ring critical point and natural population analysis charges.

Keywords Magnesium bond · Lithium bond · Lithium amide · Electrostatic interaction · Cooperative · Theoretical calculation

Introduction

Recently, intermolecular interactions involving metals have received much attention due to their potential applications in chemical reactions [1], crystal engineering [2], and biological processes [3]. Brammer presented a view of the varied roles that metals, particularly transition metals, can play in hydrogen bonding, and the potential importance and applications of metal involvement [4]. The same author also focused on inorganic components, or at least metal-containing components, and explored their propensity to form halogen bonds [5].

Lithium bonding is a strong interaction between a lithium-containing molecule (a Lewis acid) and a region of negative electrostatic potential on another molecule (a Lewis base) [6–9]. An early pioneering theoretical study on lithium bonding was performed by Kollman and coworkers [9]. Lithium and hydrogen bonding do have certain analogous features, such as charge transfer, but the electrostatic contributions and the bonding energies are considerably greater for lithium bonds [10]. Like hydrogen bonds, the electron donor in lithium bonds is also classified into lone pair electrons, π electrons, radicals [6], sigma electrons [8], and carbenes [11]. Thus, lithium bonds are of great importance in many fields. In their book "*Lithium Chemistry: A Theoretical and Experimental Overview*", Sapse and Schleyer [12] review the bonding, structures, and energies of lithium bonds involved with organolithium compounds and inorganic lithium salts.

Lithium amide ($LiNH_2$) is a new candidate for reversible hydrogen storage materials [13]. However, its 300 °C temperature of hydrogen desorption is too high for practical vehicular application. Fortunately, the temperature of hydrogen desorption for $LiNH_2$ can be decreased to 150 °C through mixing it with LiH [14]. To improve the thermodynamic properties of $LiNH_2$, a ball-milled mixture of ($LiNH_2$+MgH_2) was proposed [15, 16]. A recent paper [17] suggested that the mechanism of $LiNH_2$ and MgH_2 interactions was through lithium bonding with the Li atom in $LiNH_2$ and the H atom in MgH_2.

Here, we reinvestigate the interaction between $LiNH_2$ and MgH_2 using quantum chemical calculations. Using theoretical calculations, Yanez et al. [18] investigated a

X. Yang · Q. Li (✉) · J. Cheng · W. Li
The Laboratory of Theoretical and Computational Chemistry, Chemistry and Chemical Engineering College, Yantai University, Yantai 264005, People's Republic of China
e-mail: liqingzhong1990@sina.com

series of complexes between BeX_2 (X=H, F, Cl, OH) and different Lewis bases. A beryllium bond exists in these complexes. This beryllium bond shares many common features with hydrogen binding, but is in general significantly stronger than hydrogen binding. Considering that Mg is the same group as Be, and that Mg in MgH_2 is a more reactive metal than Be in BeH_2, we think that the Mg atom in MgH_2 can interact with the N atom in $LiNH_2$ through a Mg···N interaction. We also study the substitution effects on the complex by replacing one H atom in MgH_2 with either F, Cl, Br, CH_3, OH, or NH_2. The resulting complexes were analyzed with natural bond orbital (NBO) and atoms in molecules (AIM) methods.

Computational details

The structures of the monomers and complexes were optimized at the MP2/6-311++G(d,p) level. Frequency calculations were then carried out to confirm that the optimized structures are local minima on their potential surfaces. The optimization and frequency calculations were performed using GAUSSIAN-09 [19]. The interaction energy was calculated to be the difference between the energy of the complex and the energy sum of the monomers. The basis-set superposition error (BSSE) was eliminated from the interaction energy with the standard counterpoise correction method of Boys and Bernardi [20]. A single-point calculation was also carried out at the CCSD/6-311++G(d,p) level on the MP2 geometry. NBO analysis [21] was performed via the procedures contained within GAUSSIAN 09. Electron densities were analyzed using AIM methodology with the program AIM2000 [22]. The electrostatic potentials on the Mg atom in the complexes were calculated at the MP2/6-311++G(d,p) level with the Wave Function Analysis (WFA) Surface analysis suite [23].

Results and discussion

Geometrics

Figure 1 presents the optimized structures of $LiNH_2$–MgHX (X=H, F, Cl, Br, CH_3, OH, and NH_2) complexes. The respective bond lengths and bond angles are summarized in Table 1. Clearly, the structures of the segments in the complex change considerably. $LiNH_2$ is a planar structure as a monomer but has a nonplanar structure in the complex. Monomeric HMgX is linear but the complex is nonlinear. This indicates that there is a strong interaction between both monomers. The H–Mg–X angle is in a range of 132–135° in the complex and varies little for the different X substituents. The Li–N–Mg angle is about 81° for each complex.

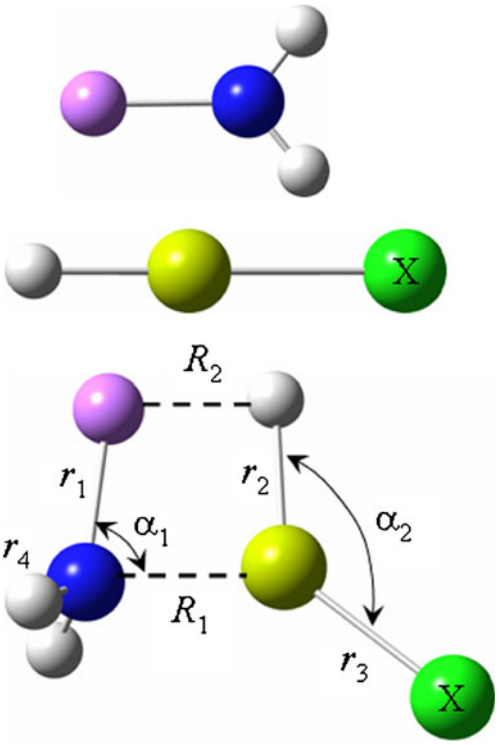

Fig. 1 Structures of the $LiNH_2$–MgHX (X=H, F, Cl, Br, CH_3, OH, and NH_2) complex and respective monomers

The distance between the Mg and N atoms is in the range of 2.070–2.103 Å, which is much smaller than the 2.7 Å sum of the van der Waals radii of the respective atoms, and is close to the length of a typical N–Mg bond. This shows that there is an attractive force between the Mg and N atoms, and that it can be referred to a magnesium bond as in the case of the beryllium bond [18]. The N···Mg distance in the $LiNH_2$–MgH_2 complex decreases when a H atom in MgH_2 is replaced with F, Cl, Br, OH, and NH_2 substituents, while the methyl substitution has a negligible elongation effect. In the $LiNH_2$–MgH_2 complex, the Li···H distance is 1.676 Å, which is also much smaller than the sum of the van der Waals radii of Li and H atoms (about 3.0 Å). So, substitution has an inverse effect on the Li···H and N···Mg distances. This indicates that a lithium–hydride interaction is present in the complex [17]. Thus the $LiNH_2$–MgHX complex displays a cyclic structure through both types of interactions. The formation of the cyclic complex can also be affirmed by the presence of ring critical point in the complex shown in Fig. 2. It was shown that the cyclic structure is more stable than the chain structure [24], thus we think that the cyclic $LiNH_2$–MgH_2 complex is mainly responsible for the mechanism for producing hydrogen in the ball-milled mixture of ($LiNH_2$+MgH_2).

Upon complexation, all the initial bonds in both monomers are elongated. The elongations of the N–Li and Mg–H bonds are larger than those for the Mg–X and N–H bonds.

Table 1 Binding distances (R, Å), changes in bond lengths (Δr, Å), and bond angles (α, degree) in the complexes

	R_1	R_2	Δr_1	Δr_2	Δr_3	Δr_4	α_1	α_2
$LiNH_2$–MgH_2	2.101	1.767	0.169	0.165	0.017	0.002	80.8	133.2
$LiNH_2$–MgHF	2.077	1.783	0.179	0.153	0.014	0.002	80.6	131.9
$LiNH_2$–MgHCl	2.070	1.786	0.180	0.147	0.021	0.002	80.6	131.8
$LiNH_2$–MgHBr	2.070	1.789	0.180	0.145	0.028	0.002	80.6	132.2
$LiNH_2$–$MgHCH_3$	2.103	1.763	0.167	0.167	0.013	0.003	80.8	132.3
$LiNH_2$–MgHOH	2.081	1.778	0.173	0.164	0.047	0.002	80.7	135.0
$LiNH_2$–$MgHNH_2$	2.090	1.774	0.174	0.160	0.013	0.002	80.3	132.2

N–Li and Mg–H bond elongation is very prominent, and their elongations are 0.17–0.18 and 0.14–0.17 Å, respectively. N–Li bond elongation becomes larger for the F, Cl, Br, OH, and NH_2 substituents but is a little smaller for the methyl substitution. The substituents have the opposite effect on the Mg–H bond elongation. The smallest elongation of the Mg–H bond is found in the $LiNH_2$–MgHBr complex, while the largest is observed in $LiNH_2$–$MgHCH_3$. The H and Mg atoms in MgHX play different roles in the Li···H and Mg···N interactions. The former acts as the Lewis base in the lithium bond, whereas the latter acts as the Lewis acid in the magnesium bond. The substituent X has a reverse effect on the H and Mg atoms in MgHX, thus the change of N–Li and Mg–H bond elongation is different for the substitutent.

Interaction energies

Determining the interaction energy is one of the most powerful methods of evaluating intermolecular interactions. Table 2 presents the interaction energies for the seven complexes. The energies of the monomers in their pre-complex geometries were used to calculate the interaction energies. The interaction energies were obtained using the two methods of MP2 and CCSD. The CCSD results were obtained by a single-point energy calculation on the MP2 geometry. These interaction energies were corrected with BSSE. The BSSE is in the range of 3.5–4.9 kcal mol^{-1}, less than 7 % of the raw interaction energy. This proportion is much smaller for the complexes than that in hydrogen binding due to the stronger strength of the Mg···N interaction. The MP2 values are almost equal to the CCSD values for the same reason.

The MP2 interaction energies vary from −63.2 to −66.5 kcal mol^{-1}, which is much larger than those in dihydrogen bond [25] and lithium bond [26]. This is because two strong interactions are present in these complexes. For the H_2LiN–MgH_2 complex, another structure (Fig. 3) was also optimized although one imaginary frequency is calculated for this structure. In this structure, only one Mg···N interaction is present and the respective interaction energy is −40.1 kcal mol^{-1}. If only one Li···H interaction is present between H_2LiN and MgH_2, the interaction energy is −12.5 kcal mol^{-1} [17]. The sum of the interaction energy for both types of interactions is smaller than −63.7 kcal mol^{-1} in the H_2LiN–MgH_2 complex. This indicates that a cooperative

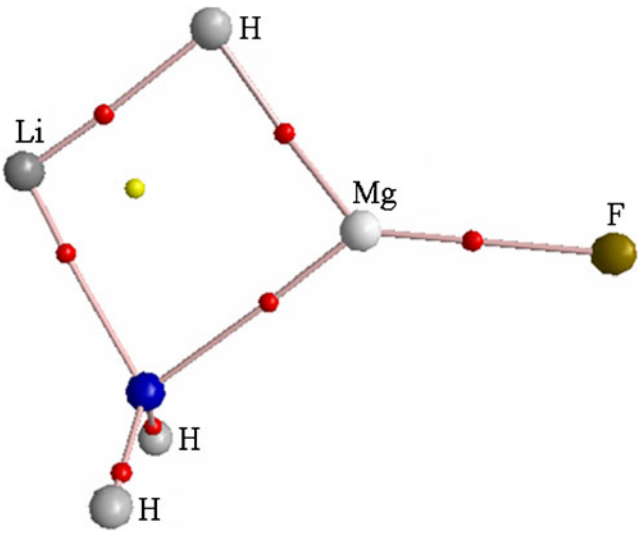

Fig. 2 Molecular graph of $LiNH_2$–MgHF complex at the MP2/6-311++G(d,p) level. *Small red balls* Bond critical points, *small yellow ball* ring critical point

Table 2 Interaction energy (ΔE, kcal mol^{-1}) corrected for basis-set superposition error (BSSE) in the complexes at the MP2/6-311++G(d,p) and CCSD/6-311++G(d,p) levels

	ΔE_{MP2}	BSSE	ΔE_{MP2}^{CP}	ΔE_{CCSD}^{CP} [a]
$LiNH_2$-MgH_2	−67.2	3.5	-63.7	-63.4
$LiNH_2$-MgHF	−70.4	4.2	-66.2	-66.3
$LiNH_2$-MgHCl	−71.4	4.9	-66.5	-66.4
$LiNH_2$-MgHBr	−70.8	4.3	-66.5	-66.4
$LiNH_2$-$MgHCH_3$	−67.1	3.9	-63.2	-63.2
$LiNH_2$-MgHOH	−69.3	4.2	-65.1	-65.1
$LiNH_2$-$MgHNH_2$	−69.0	4.0	-65.0	-65.1

[a] Obtained with a single-point calculation at the CCSD level on the MP2 geometry

effect exists between the Mg···N and Li···H interactions in the $H_2LiN–MgH_2$ complex as between hydrogen binding [27–29]. Such cooperativity is also reflected in the change in the binding distance. The N···Mg distance in Fig. 1 (2.070–2.103 Å) is smaller than that in Fig. 3 (2.124 Å).

The interaction energy in the $H_2LiN–MgH_2$ complex is much bigger in magnitude than −13.1 kcal mol^{-1} in the HMgH–LiH complex [8]. In our previous study of dimethyl sulfoxide–methanol complexes [30], we pointed out that the methyl group in the proton acceptor (dimethyl sulfoxide) and the proton donor (methanol) plays a positive role in the formation of the O···HO hydrogen binding. But for the complex here, the methyl group in $MgHCH_3$ plays the opposite role, although its effect is small. For other substituents, whether electron-donating groups or electron-withdrawing groups, the interaction energies become more negative. This substitution effect is different from that in hydrogen binding [31]. A further analysis shows that a linear relationship is present between the interaction energy and the binding distance in these complexes.

The complexes of LiX (X=H, F, Cl, Br, OH, NH_2) and $HMgNH_2$, with X bridging the two metals, were also studied. The related structures are shown in Fig. 4. Two configurations (I and II) were found: configuration I with NH_2 as an additional bridge, and configuration II with H as an additional bridge. The structure of $HMgNH_2$ shows a prominent change in the complexes with respect to the isolated molecule. In the monomer, the three atoms (N, Mg, and H) are in a line, while the H atom deviates from the line in the complex. The deviation is a little larger in configuration II. The NH_2 structure in configuration II is similar to that in the monomer, while it is not a planar structure in configuration I due to the repulsive interaction between the positive H and Li atoms. Their interaction energies are listed in Table 3.

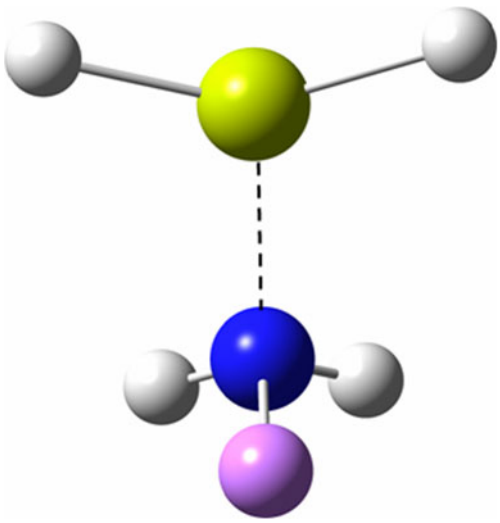

Fig. 3 Optimized structure of $LiH_2N–MgH_2$ complex with one imaginary frequency

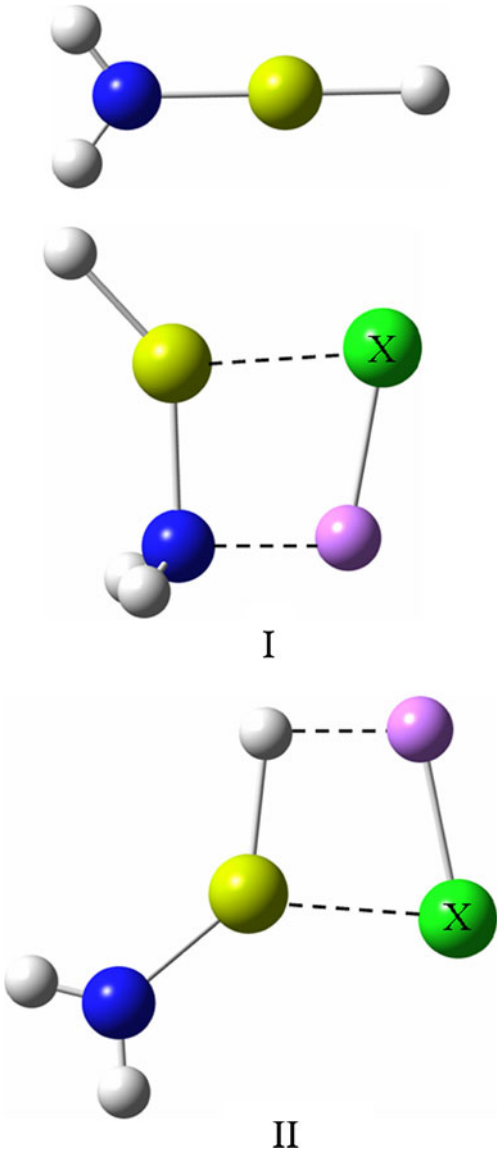

Fig. 4 Structures of $LiX–MgHNH_2$ (X=H, F, Cl, Br, OH, and NH_2) complexes and $MgHNH_2$ monomer

The interaction energy of configuration I was found to be more stable than that of configuration II. Two types of interaction are present in both configurations: a Mg···X

Table 3 Interaction energy (ΔE, kcal mol^{-1}) corrected for BSSE in the complexes at the MP2/6-311++G(d,p) level

	ΔE		ΔE
$LiH-MgHNH_2$-I	−67.3	$LiH-MgHNH_2$-II	−53.9
$LiF-MgHNH_2$-I	−70.7	$LiF-MgHNH_2$-II	−57.4
$LiCl-MgHNH_2$-I	−60.3	$LiCl-MgHNH_2$-II	−47.1
$LiBr-MgHNH_2$-I	−59.6	$LiBr-MgHNH_2$-II	−46.1
$LiHO-MgHNH_2$-I	−76.1	$LiHO-MgHNH_2$-II	−63.1
$LiH_2N-MgHNH_2$-I	−77.5	$LiH_2N-MgHNH_2$-II	−65.0

Table 4 Charge on the atoms (q, e), Wiberg BO associated with the Mg···N and Li···H interactions, and the most positive electrostatic potential on the Mg atom surface (V_{max}, eV) of MgHX in the complexes

Complex	q_N	q_{Mg}	q_{Li}	q_H	$BO_{Mg\cdots N}$	$BO_{Li\cdots H}$	V_{max}
$LiNH_2$-MgH_2	-1.518	1.261	0.831	-0.667	0.22	0.16	0.24
$LiNH_2$-MgHF	-1.540	1.572	0.831	-0.697	0.21	0.17	0.31
$LiNH_2$-MgHCl	-1.524	1.370	0.840	-0.669	0.24	0.15	0.29
$LiNH_2$-MgHBr	-1.523	1.317	0.842	-0.664	0.24	0.15	0.28
$LiNH_2$-$MgHCH_3$	-1.514	1.375	0.826	-0.671	0.23	0.17	0.23
$LiNH_2$-MgHOH	-1.529	1.563	0.828	-0.689	0.22	0.17	0.31
$LiNH_2$-$MgHNH_2$	-1.518	1.464	0.830	-0.677	0.23	0.17	0.29

interaction and a lithium bond. The latter is a conventional lithium bond with N as the lithium acceptor in configuration I but a lithium-hydride lithium bond with the negative H as the lithium acceptor in t configuration II. It has been demonstrated that conventional lithium bonds are stronger than lithium-hydride lithium bonds [8, 32]. The interaction energy is less than −16 kcal mol^{-1} for the lithium-hydride lithium bond [8]. The interaction energy has a similar change in both configurations. In the LiH-$MgHNH_2$ structure, the negative H atom in LiH is associated with the positive Mg in $MgHNH_2$. The role of the negative H atom in this complex is like that in the dihydrogen bond [25] and the lithium-hydride lithium bond [8]. If the contribution of the lithium-hydride lithium bond is removed from the LiH–$MgHNH_2$-II complex, the magnesium-hydride magnesium bond is stronger than the dihydrogen bond and lithium-hydride lithium bond. If the negative H atom is replaced with an F, OH, or NH_2 group, the magnesium bond becomes stronger and its strength increases in order of F<OH<NH_2, which is consistent with their electronegativity. If the negative H atom is replaced with other halogen atoms, the magnesium bond becomes weaker. All changes are similar to those in hydrogen bonds. Configuration II is less stable than the $LiNH_2$–MgHX structure (Fig. 1), with the difference being very small for X=OH and NH_2 but larger for X= H, F, Cl, and Br. Configuration I is more stable than the $LiNH_2$–MgHX structure when X is H, F, OH, and NH_2, while it is less stable than the $LiNH_2$–MgHX structure when X is Cl or Br.

Table 5 Electron densities (ρ, au) and Laplacians ($\nabla^2\rho$, au) at the bond critical points (BCPs) in the complexes

Complex	$\rho_{N\cdots Mg}$	$\rho_{Li\cdots H}$	$\nabla^2\rho_{N\cdots Mg}$	$\nabla^2\rho_{Li\cdots H}$
$LiNH_2$-MgH_2	0.0426	0.0265	0.2855	0.1191
$LiNH_2$-MgHF	0.0451	0.0255	0.3067	0.1155
$LiNH_2$-MgHCl	0.0459	0.0254	0.3134	0.1149
$LiNH_2$-MgHBr	0.0460	0.0252	0.3132	0.1142
$LiNH_2$-$MgHCH_3$	0.0425	0.0267	0.2839	0.1200
$LiNH_2$-MgHOH	0.0477	0.0257	0.3030	0.1163
$LiNH_2$-$MgHNH_2$	0.0437	0.0261	0.2951	0.1173

NBO and AIM analyses

For a better understanding of the formation of the complexes, NBO and AIM analyses were carried out. The results are summarised in Tables 4 and 5, respectively. The charges on the N and H atoms are negative, whereas the charges on the Mg and Li atoms are positive. These charges are so large that it is reasonable to think that the electrostatic interaction plays a dominant role in stabilizing the complexes. In the case of the beryllium bond, there is a dominant electrostatic character although there is a non-negligible electron transfer between the interacting subunits [18]. It has been demonstrated that the lithium-bonded complexes are dominated by electrostatic interactions [6–11]. These results support the above conclusion concerning the complexes reported here. The negative charge on the N atom in the $LiNH_2$–MgH_2 complex increases in magnitude due to the substitutent effects, except for the methyl substitution. All substituents lead to a substantial increase in the positive charge on the Mg atom in the $LiNH_2$–MgHX complex. The positive charge on the Li atom and the negative charge on the H atom also increase in most complexes. The Wiberg BO for the Mg–N bond is greater than that for the Li–H bond in each complex.

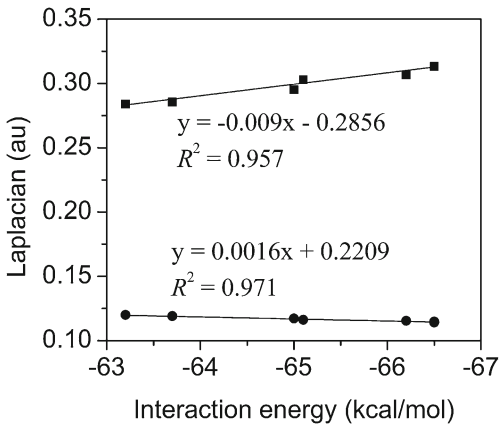

Fig. 5 Relationship between the interaction energy and Laplacian at the Mg···N (■) and Li···H (●) BCPs

The electrostatic potentials on the Mg atom in the complexes were also considered. One can see from Table 4 that the Mg atom shows a positive electrostatic potential, indicating its role as a Lewis acid in the Mg···N interaction. The most positive electrostatic potential on the Mg atom exhibits a similar change with the interaction energy, showing the contribution of the electrostatic interaction in the Mg···N interaction.

Bader's AIM theory is also a useful tool for confirming the existence of the magnesium and lithium bonds in these complexes. Mg···N and Li···H bond critical points (BCPs) shown in Fig. 2 were probed in each complex. The calculated electron density (ρ) and its Laplacian ($\nabla^2\rho$) are presented in Table 4. It can be seen that the value of ρ at the Mg···N BCP varies from 0.0425 to 0.0477 au and the respective $\nabla^2\rho$ is within a range of 0.2839–0.3134 au. The electron density associated with the Mg···N BCP is typical of the interactions between closed shell systems but larger than those found in conventional hydrogen binding [33]. The values for both the electron density and its Laplacian at the Mg···N BCP exceed the range of hydrogen binding proposed by Koch and Popelier [33]. It shows that the Mg···N interaction is far stronger than hydrogen binding. The values for both the electron density and its Laplacian at the Li···H BCP are in the range of hydrogen binding proposed by Koch and Popelier [33], and are much smaller than those at the Mg···N BCP. This means that the lithium bond is weaker than the magnesium bond in the complex. Figure 5 shows the relationship between the interaction energy and the electron density at the BCPs. It can be concluded from the figure that, with the increase of the interaction energy, the Laplacian at the Mg···N BCP increases, while the Laplacian at the Li···H BCP decreases. Clearly, the former has a larger change than the latter, indicating that the substituents have a bigger effect on the magnesium bond than on the lithium bond.

Conclusions

Complexes of $LiNH_2$ and HMgX (X=H, F, Cl, Br, CH_3, OH, and NH_2) are stabilized through the combinative interaction of a magnesium bond and a lithium bond simultaneously. The cyclic structure of the complexes is characterized with the presence of a ring critical point in each complex. The interaction energies are in the range of 63.2–66.5 kcal mol^{-1}, which is much greater than that of hydrogen binding or lithium binding. The cooperative effect is found for the Mg···N bond and Li···H interactions. As the complex forms, both Mg–H and Li–N bonds are lengthened. The substituents have a reverse effect on the Mg–H and Li–N bond elongation. We think that the cyclic $LiNH_2$–MgH_2 complex is mainly responsible for the mechanism for producing hydrogen in the ball-milled mixture of ($LiNH_2$+MgH_2).

Acknowledgments This work was supported by the National Natural Science Foundation of China (20973149), the Outstanding Youth Natural Science Foundation of Shandong Province (JQ201006), the Excellent Young Scientist Research Foundation of Shandong Province (2009BSD01587) and the Program for New Century Excellent Talents in University. The authors thank Prof. Robert E. Loffredo for his assistance in writing this letter.

References

1. Shi FQ, Li X, Xia YX, Zhang LM, Yu ZX (2007) J Am Chem Soc 129:15503–15512
2. Burrows AD, Harrington RW, Mahon MF (2000) Cryst Eng Commun 2:77–81
3. Dudev T, Lim C (2008) Annu Rev Biophys 37:97–116
4. Brammer L (2003) Dalton Trans 16:3145–3157
5. Brammer L, Espallargas GM, Libri S (2008) Cryst Eng Commun 10:1712–1727
6. Li Y, Wu D, Li ZR, Chen W, Sun CC (2006) J Chem Phys 125:084317
7. Feng Y, Liu L, Wang JT, Li XS, Guo QX (2004) Chem Commun 88–89
8. Li QZ, Wang YF, Li WZ, Cheng JB, Gong BA, Sun JZ (2009) Phys Chem Chem Phys 11:2402–2407
9. Kollman PA, Liebman JF, Allen LC (1970) J Am Chem Soc 92:1142–1150
10. Sannigrahi AB, Kar T (1990) Guha Niyogi B, Hobza P, Schleyer PvR. Chem Rev 90:1061–1076
11. Li QZ, Wang HZ, Liu ZB, Li WZ, Cheng JB, Gong BA, Sun JZ (2009) J Phys Chem A 113:14156–14160
12. Sapse AM, PvR S (1995) Lithium chemistry: a theoretical and experimental overview. Wiley, New York
13. Chen P, Xiong Z, Luo J, Lin J, Tan KL (2002) Nature 420:302–304
14. Chen P, Xiong Z, Luo J, Lin J, Tan KL (2003) J Phys Chem B 107:10967–10970
15. Barison S, Agresti F, LoRusso S, Maddalena A, Palade P, Principi G, Torzo G (2008) J Alloys Comp 459:343–347
16. Ichikawa T, Isobe S, Hanada N, Fujii H (2004) J Alloys Comp 365:271–276
17. Wang WJ, Li WJ, Li QZ (2011) Int J Quant Chem 111:675–681
18. Yanez M, Sanz P, Mo O, Alkorta I, Elguero J (2009) J Chem Theor Comput 5:2763–2771
19. Frisch MJ, Trucks GW, Schlegel HB, Scuseria GE, Robb MA, Cheeseman JR, Scalmani G, Barone V, Mennucci B, Petersson GA, Nakatsuji H, Caricato M, Li X, Hratchian HP, Izmaylov AF, Bloino J, Zheng G, Sonnenberg JL, Hada M, Ehara M, Toyota K, Fukuda R, Hasegawa J, Ishida M, Nakajima T, Honda Y, Kitao O, Nakai H, Vreven T, Montgomery JA, Peralta JE, Ogliaro F, Bearpark M, Heyd JJ, Brothers E, Kudin KN, Staroverov VN, Kobayashi R, Normand J, Raghavachari K, Rendell A, Burant JC, Iyengar SS, Tomasi J, Cossi M, Rega N, Millam JM, Klene M, Knox JE, Cross JB, Bakken V, Adamo C, Jaramillo J, Gomperts R, Stratmann RE, Yazyev O, Austin AJ, Cammi R, Pomelli C, Ochterski JW, Martin RL, Morokuma K, Zakrzewski VG, Voth GA, Salvador P, Dannenberg JJ, Dapprich S, Daniels AD, Farkas O, Foresman JB, Ortiz JV, Cioslowski J, Fox DJ (2009) Gaussian09, Revision A.02. Gaussian Inc, Wallingford, CT
20. Boys SF, Bernardi F (1970) Mol Phys 19:553–566
21. Reed AE, Curtiss LA, Weinhold FA (1988) Chem Rev 88:899–926

22. Biegler-König F (2000) AIM2000. University of Applied Sciences, Bielefeld
23. Bulat FA, Toro-Labbé A, Brinck T, Murray JS, Politzer P (2010) J Mol Model 16:1679–1691
24. Kirchner B, Reiher M (2002) J Am Chem Soc 124:6206–6215
25. Grabowski SJ (2000) J Phys Chem A 104:5551–5557
26. Yin JG, Wei P, Li QZ, Liu ZB, Li WZ, Cheng JB, Gong BA (2009) J Mol Struct: THEOCHEM 916:28–32
27. Kar T, Scheiner S (2004) J Phys Chem A 108:9161–9168
28. Rivelino R, Canuto S (2001) J Phys Chem A 105:11260–11265
29. Li QZ, An XL, Gong BA, Cheng JB (2007) J Phys Chem A 111:10166–10173
30. Li QZ, Wu GS, Yu ZW (2006) J Am Chem Soc 128:1438–1439
31. Scheiner S, Grabowski SJ, Kar T (2001) J Phys Chem A 105:10607–10612
32. Szczesniak MM, Ratajczak H (1980) Chem Phys Lett 74:243–247
33. Koch U, Popelier PLA (1995) J Phys Chem A 99:9747–9754